Synthetic Metals 294 (2023) 117308

Contents lists available at ScienceDirect

Synthetic Metals

journal homepage: www.elsevier.com/locate/synmet

Construction of electroactive polyamine-enzyme assemblies nondependent on the electrical charge

Lucy L. Coria-Oriundo [a], M. Lorena Cortez [b], Santiago E. Herrera [a], Omar Azzaroni [b], Fernando Battaglini [a,*]

[a] INQUIMAE (CONICET), Departamento de Química Inorgánica, Analítica y Química Física, Facultad de Ciencias Exactas y Naturales, Universidad de Buenos Aires, Ciudad Universitaria, Pabellón 2, C1428EHA Buenos Aires, Argentina
[b] Instituto de Investigaciones Fisicoquímicas Teóricas y Aplicadas (INIFTA), Departamento de Química, Facultad de Ciencias Exactas, Universidad Nacional de La Plata, CONICET, Sucursal 4, Casilla de Correo 16, 1900 La Plata, Argentina

ARTICLE INFO

Keywords:
Electrical charge nondependent assemblies
Redox polyamine
Hydrogen bond crosslinker
Redox active particles

ABSTRACT

The assembly of polyelectrolytes and biomacromolecules (proteins, DNA) has attracted great attention in several fields related to medicine, molecular biology, and clinical chemistry. Here, a quick and easy multicomponent self-assembly is used to unite two species with the same charge to form an electroactive polyamine-enzyme assembly. Phosphate ions are added as a crosslinker agent to create a stable structure. Osmium-derivatized polyallylamine is combined with horseradish peroxidase (pI = 8.6) or PQQ-glucose dehydrogenase (pI = 9.5) on graphite electrodes. The assemblies are built by layer-by-layer or one-pot deposition. In both cases, the electrocatalytical signals observed are comparable to the state-of-the-art results. The proposed construction method represents a new alternative for the assembly of polyamines with proteins independently of their charge.

1. Introduction

The association between charged biomacromolecules and synthetic polymers is generally attributed to electrostatic interactions. Even though this is an important driving force from a kinetics point of view, the association of charged macromolecules is a more complex phenomenon involving an entropic component, the loss of counterions, and forces beyond the electrostatic interactions, like van der Waals and hydrogen binding forces [1–3].

The layer-by-layer (LbL) technique enables the creation of multilayered structures in which the adsorbed materials can be finely controlled, resulting in an improvement in the performance of the desired device. Due to the ability to control the architecture and maintain the enzyme activity, the assembly of electroactive polyelectrolytes, nanomaterials, and redox enzymes has been extensively exploited in different scenarios, ranging from bioelectrochemistry [4–7] and bioelectronics to nanofluidic sensing [8–12]. However, as shown by the references included in recent reviews, [13,14] the majority of assemblies are restricted to electrostatic interactions. Another technique used is the addition of nanomaterials to enhance the functionality of the intended device, as demonstrated, for instance, by Zhang et al. in their work on the application of LbL assemblies to enzymatic biofuel cells [15]. An interesting method to go around the counter charge limitation was developed by the group of Gillian-Dupont, where the enzyme is wrapped with a polyelectrolyte of opposite charge, therefore it can be later assembled with a polyelectrolyte of the same charge. For example, positively charged lysozyme forms a complex with negatively charged heparin, and the complex can be assembled on a surface with positively charged chitosan [16]. Although this represents a step forward in the assembly of enzymes with polyelectrolytes, it has some limitations in bioelectrochemical applications because both polyelectrolytes must be derivatized with electroactive moieties.

Polyamines are a class of weak polyelectrolytes that can change their charge at different pHs, interact with phosphate through hydrogen bonding allowing the formation of three-dimensional structures [17–23] and change their hydrophilic/hydrophobic characteristics depending on the ions present in solution through ion-pairing association [24]. Finally, the amino group can be easily modified in nature by the conjugation of biogenic oligoamines in plants [25] and by synthetic means by introducing new functionalities and generating new materials to address current challenges in energy, health, and sustainability [26–29]. Electroactive conjugated polyamines have been used in several

* Corresponding author.
E-mail address: battagli@qi.fcen.uba.ar (F. Battaglini).

https://doi.org/10.1016/j.synthmet.2023.117308
Received 20 November 2022; Received in revised form 25 January 2023; Accepted 16 February 2023

applications, including the creation of redox enzyme-based biosensors [30] and the comprehension of the electron transfer mechanism in modified electrodes [31]. However, most of these systems are constructed through covalent crosslinking or LbL assembly exploiting the opposite charge of the redox enzyme. Examples of polyamines used in bioelectrochemistry are polyallylamine, [5,32] polyelthyleneimine, [33, 34] polyvynilimidazole, [35] polyvinylpyridine, [36,37] and chitosan [38]. However, from the characteristics previously described, different approaches can be explored considering the malleability of polyamines to improve the current generation of the electroactive polyamine–redox enzyme system, in this respect we have shown the ability of hydrophobic ions to improve the adsorption of glucose oxidase on electroactive polyethyleneimine and polyallylamine [24].

A strategy that merits consideration is looking for the assembly of polyamines and redox enzymes that have the same charge because it will broaden the range of feasible configurations. In this work we show how using soft nanoparticles generated by the interaction of osmium complex-based polyallylamine with phosphate ions can assemble redox protein positively charged (horseradish peroxidase and PQQ-glucose dehydrogenase) through noncovalent interactions that shows competitive electrocatalytical signals.

2. Experimental

Materials: $OsCl_6(NH_4)_2$, pyridine aldehyde (pyCHO), sodium cyanoborohydride (cat #156159), and polyallylamine (cat #479136) were procured from Sigma Aldrich; 2,2′-bipyridine (bpy) was provided by Fluka. Glucose dehydrogenase PQQ-dependent (GDH) was procured from Sorachim SA and Horseradish peroxidase (HRP) from Calzyme Laboratories, Inc. All other reagents were of analytical grade. Ultrapure water (18 MOhm) was used to prepare the solutions. The osmium-modified polyallylamine (OsPAA) was synthetized as previously reported [24].

Enzyme's isoelectric points: They were determined by isoelectric focusing analysis in PhastSystem Equipment (Amersham Biosciences, Uppsala, Sweden) [39].

Electrochemical measurements: A screen-printed three electrode system with graphite working electrodes was used [40]. For the layer-by-layer electrode modification OsPAA was dissolved in a final osmium concentration of 0.57 mM in the matrices listed in Table 1, while 2 mg mL^{-1} enzyme (GDH or HRP) was dissolved in water pH 6.1. Electrodes were modified following the procedure previously described by Coria-Oriundo et al.[34] For one-pot drop-casting experiments, the enzyme was added to the OsPAA solutions at a final concentration of 2 mg mL^{-1}. Electrodes were modified following the procedure previously described by Coria-Oriundo et al. [34].

Electrochemical Impedance Spectroscopy (EIS) measurements was performed in used the modified electrodes with OsPAA/GDH assemblies. Frequencies from 1 Hz to 50 kHz with an amplitude of 10 mV around E° were applied. Electrodes were immersed in 50 mM Buffer HEPES + 0.1 M NaCl, pH 7 solution. EIS Spectrum Analyser (EISSA) software (http://www.abc.chemistry.bsu.by/vi/analyser/) was used for data processing.

Quartz Crystal Microbalance Measurements: The quartz crystal microbalance with dissipation (QCM-D) experiments were performed for layer-by-layer assemblies, using OsPAA and GDH solutions as described for electrode modification, following a procedure previously reported [41].

Dynamic Light Scattering Measurements: The hydrodynamic diameter and z-potential of the colloids were determined by Dynamic Light Scattering employing a Zetasizer Nano as described previously [34].

Atomic Force Microscopy: An Agilent 5500 at. force microscope/scanning probe microscope was used for atomic force microscopy (AFM). Contact mode and tapping mode measurements were carried out using insulating Si PointProbe Plus PPP-CONT tips (<10 nm tip radius, a force constant of 0.2 N/m, a resonance frequency of 13 kHz) and PointProbe Plus PPP-NCL tips (<10 nm tip radius, a force constant of 48 N/m, a resonance frequency of 190 kHz), respectively. The topography of multilayer OsPAA/GDH was studied in the tapping mode over template-stripped (TS) gold substrates prepared as reported previously [42]. Mean film thicknesses were calculated in the contact mode by extracting a one-dimensional (1D) distribution of heights of a flattened AFM image exposing equal amounts of the surface and film and calculating the distance between the peak corresponding to the surface and the peak corresponding to the film. The roughness average parameter was calculated along an 8 μm straight line over a surface-representative AFM image. All images were analyzed using Gwyddion V2.49 (http://gwyddion.net/).

Table 1
Composition and nomenclature of matrices used on LbL assemblies.

Solution Composition[a]	Nomenclature
10 mM phosphate buffer	@Pi
10 mM phosphate buffer + 1 M NaCl	@Pi,HIS
0.2 M NaBr	@NaBr
Water	@H2O

[a]All solutions at pH 6.1

3. Results

We used layer-by-layer deposition (LbL) or one-pot drop-casting (OP) to modify graphite electrodes with an osmium polypyridyl complex modified polyallylamine (OsPAA) and an enzyme (glucose dehydrogenase PQQ-dependent (GDH) or horseradish peroxidase (HRP)) (Scheme 1). These processes allow for the formation of a supramolecular structure between a polycation and a positive charged surface enzyme at the interface of the electrode. The catalytic response of these bioelectrodes was evaluated in the presence of glucose and hydrogen peroxide, dependent on the immobilized enzyme.

3.1. Layer-by-layer assemblies (LbL)

We studied the conformational change on OsPAA in the presence of phosphate ions (10 mM, pH 6.1) at different ionic strengths (with or without 1 M NaCl) and how this affects the amount of redox cationic polymer adsorbed on the electrode surface. Then, the enzyme immobilization was carried out in water adjusted to pH 6.1, where both GDH (pI = 9.5) and HRP (pI = 8.6) have a positive charge surface.

Previous dynamic light scattering experiments of OsPAA in water or 1 M NaCl showed that the polyamine is unable to form colloid structures in these matrices.[41] Table 2 shows that the presence of phosphate ions in OsPAA solution allows for a unimodal distribution of colloidal particles with a slightly positive Z-potential. Adding 1 M NaCl, the polydispersity increases, and a bimodal distribution is obtained, showing smaller colloidal particles and the presence of free polymer. These redox particles can be adsorbed on a surface, forming a film on which an enzyme can be adsorbed.

The growth of the LbL assemblies up to four bilayers was analyzed with a quartz crystal microbalance with dissipation (QCM-D) to study the formation of the layer-by-layer assemblies, establish the adsorbed mass of the components, and determine the stiffness of the films.

In the presence of phosphate ions (Fig. 1A), the mass adsorbed increases with each layer deposition, reaching a total adsorbed mass of 23 μg cm^{-2}. In the assembly of OsPAA in the presence of both phosphate ions and 1 M NaCl, with the deposition of 2nd, 3rd and 4th OsPAA layers, the adsorbed mass decreases (Fig. 1B). This can be attributed by the removal of the loosely adsorbed material (smaller particles and/or free polymer, see Table 2) by a washing effect. The total adsorbed mass only reaches 8.5 μg cm^{-2} in the @Pi,HIS matrix.

Mass adsorbed change, dissipation change, and relative dissipation change for each layer of the assemblies OsPAA/GDH using OsPAA in

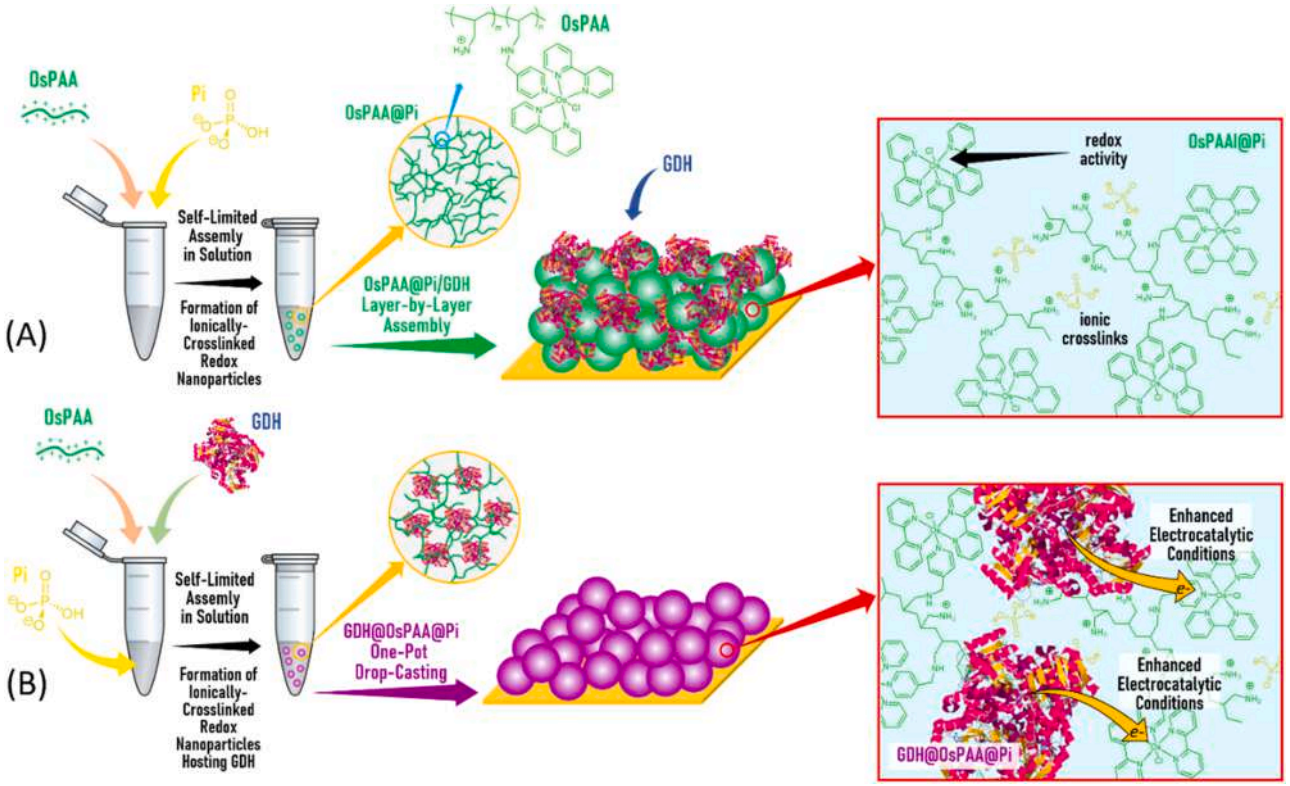

Scheme 1. Simplified general description of the electrode modification strategies implemented via different self-assembly processes: (A) layer-by-layer assembly, (B) one-pot drop-casting assembly.

Table 2
OsPAA solutions in different matrix studied by Dynamic Light Scattering (DLS).

Matrix	Diameter (nm)	PLD	Zeta potential (mV)
@Pi	580 ± 30	0.40	+ 3
@Pi,HIS	6 ± 1	0.96	+ 10
	350 ± 70		

different matrices are reported in Table 3. When the redox polymer is adsorbed on GDH, the relative dissipation has a significant increase, suggesting that OsPAA adsorbs simultaneously with a significant amount of water, producing a more flexible film. Although the amount of GDH always increases, its adsorption from the second layer produces an increase in the stiffness of the film. In the assembly with OsPAA@Pi, HIS, however, the relative dissipation changes increases slightly

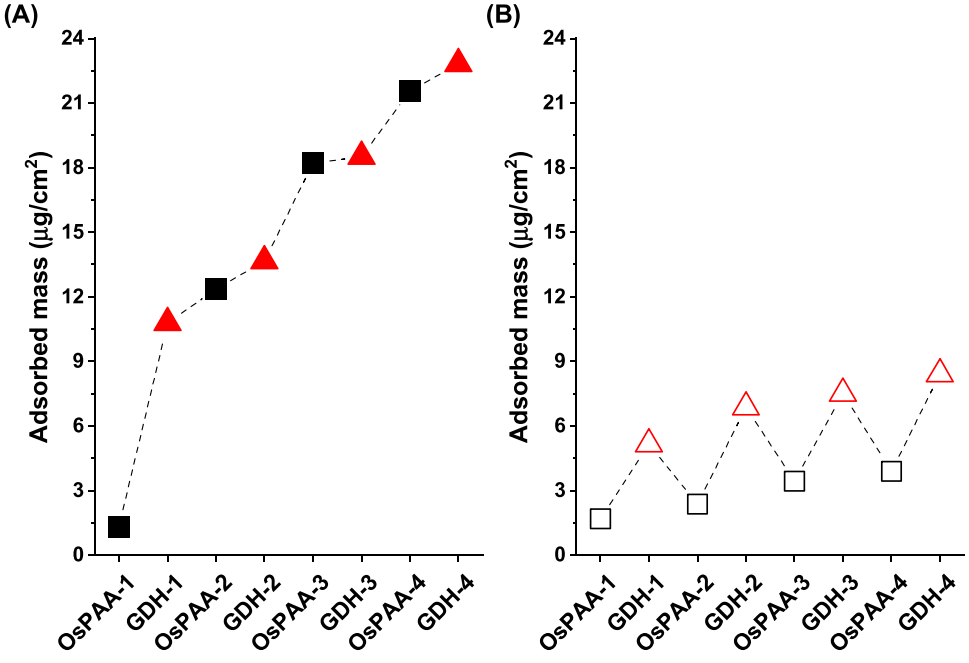

Fig. 1. QCM-D experiments: Adsorbed mass for OsPAA/GDH using (A) OsPAA@Pi or (B) OsPAA@Pi,HIS.

Table 3
Mass adsorbed change (Δm), dissipation change (ΔD) and relative dissipation change (-ΔD/ΔF) for each layer of the assemblies OsPAA/GDH using OsPAA in different matrices.

Layer	OsPAA@Pi			OsPAA@Pi,HIS		
	Δm ($\mu g\ cm^{-2}$)	ΔD (10^{-6})	-ΔD/ΔF ($10^{-6}\ Hz^{-1}$)	Δm ($\mu g\ cm^{-2}$)	ΔD (10^{-6})	-ΔD/ΔF ($10^{-6}\ Hz^{-1}$)
OsPAA-1	1.334	10	0.13	1.688	17	0.17
GDH-1	9.456	32	0.06	3.474	2	0.01
OsPAA-2	1.559[a]	115	1.31	-2.799	-3	0.02
GDH-2	1.319	-39	-0.52	4.508	66	0.26
OsPAA-3	4.537[a]	210	0.82	-3.431	-49	0.25
GDH-3	0.310	-25	-1.45	4.069	59	0.26
OsPAA-4	3.041[a]	143	0.83	-3.619	-61	0.30
GDH-4	1.258	-15	-0.21	4.519	73	0.29

a Mass adsorbed assuming Sauerbrey behavior.

regardless of whether mass is adsorbed or desorbed. Also, the mass removed by the incubation with OsPAA increases from 2nd up to 4th layer, which shows that despite GDH being adsorbed, more of it is lost as the number of bilayers increases.

Also, we performed AFM measurements over a single layer of OsPAA adsorbed over TS Au using water or phosphate as matrices (Fig. 2A). These AFM images shown a poor surface coverage for the layer adsorbed with OsPAA aqueous solution, while using OsPAA in the presence of phosphate ions, the coverage is enhanced and presents areas of greater accumulation of adsorbed material. Fig. 2B shows AFM images for the assemblies up to two bilayers with the same matrices. Here, for both systems all the gold surface was modified. However, the assembly of OsPAA in the presence of phosphate displayed grains of bigger size in comparison with using water as matrix. Furthermore, for these last systems we determined the roughness resulting in 13.4 nm and 3.3 nm for the assemblies using @Pi and @H_2O as matrix (Fig. 2C), respectively. Also, the thickness of the films obtained from the height distribution (Fig. S1) shows the formation of a thicker film when OsPAA is in the

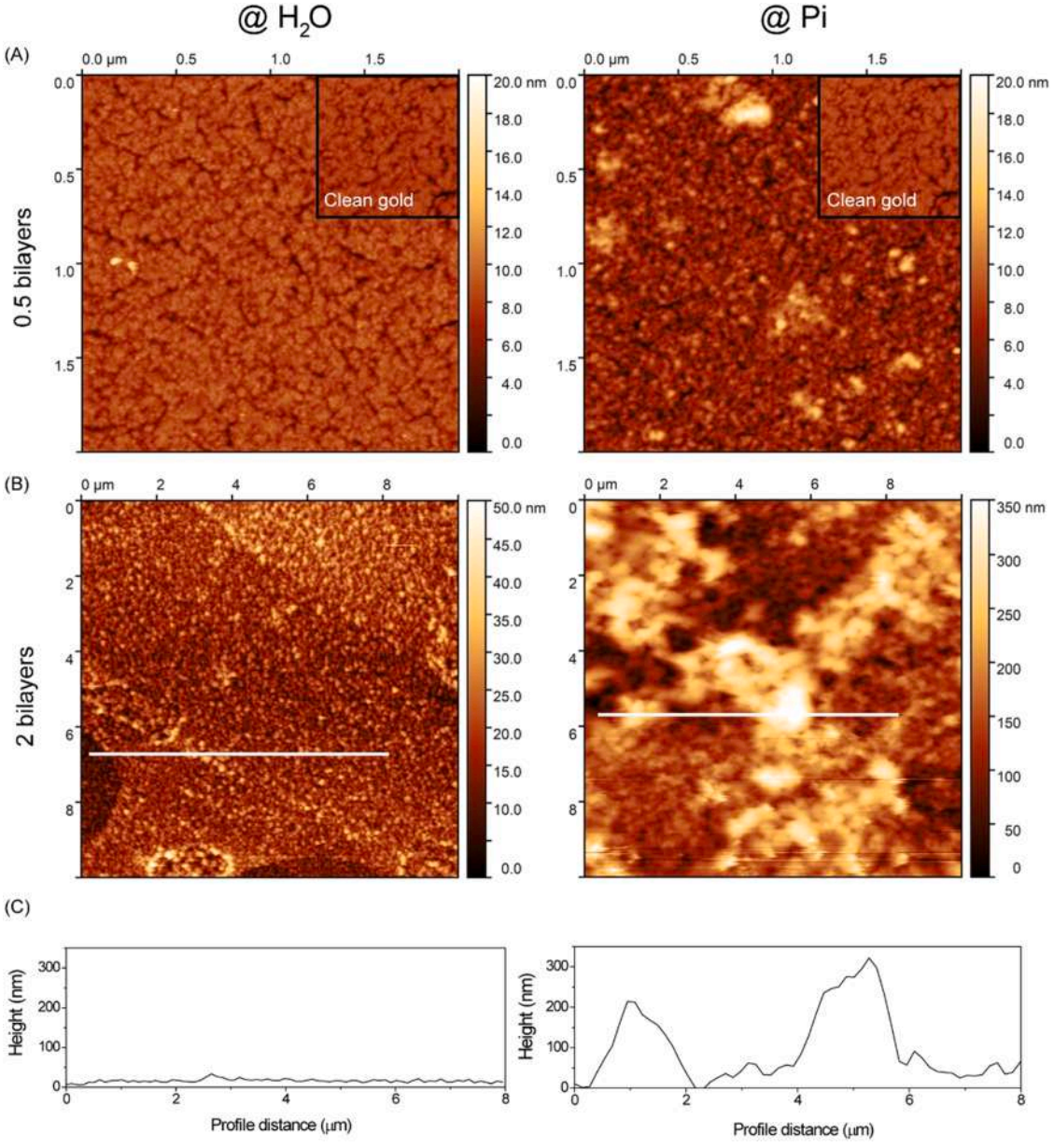

Fig. 2. AFM topography images of (A) one layer of OsPAA@X and (B) (OsPAA@X/GDH@H_2O)$_2$ over TS gold surface. (C) Height profiles corresponding to selected lines displayed over AFM images from Fig. 2B.

presence of phosphate ions (80 nm), than when it is in aqueous solution (20 nm).

The previous experiments show that an assembled LbL system is formed using OsPAA and GDH, and that the characteristics of the polymeric film depend on the matrix used. With these findings, electrode modification was carried out until four bilayers were formed; the OsPAA/GDH electrodes were tested first in the absence of enzyme substrate. The cyclic voltammetry displayed a typical response associated to a reversible redox process of the osmium centers in OsPAA (Fig. S2A).

The effect of the formation of colloidal particles with the presence of phosphate ions as well as the effect of ionic strength on the electron transfer process through the films are shown in Fig. 3 and compared with films grown in water and in a hydrophobic environment (0.2 M NaBr, @NaBr) [24]. Using water as matrix for OsPAA solutions, a slight increase in non-catalytic current densities is observed, reaching only 5.5 μA cm^{-2}, a similar behavior is observed in the presence of sodium bromide. Both systems containing phosphate show a similar increase in current densities with the number of bilayers adsorbed is observed, reaching 24 and 22 μA cm^{-2} without and with NaCl, respectively. Here, the effect due the presence of colloidal particles formed in each of these matrices in comparison with the use of an aqueous OsPAA solution (@H_2O) is noticeable. Finally, in contrast to previous results with glucose oxidase in the presence of bromide ions, [24] the polyelectrolyte-enzyme system does not show remarkable adsorption using OsPAA@NaBr.

Charge propagation in the film was studied using electrochemical impedance spectroscopy (Fig. S3). The results were analyzed considering an equivalent circuit (Fig. S3A) that includes a solution resistance (Rs), a charge transfer resistance (R_{CT}) and a Warburg element (Z_W). In parallel to the R_{CT} and the Z_W a constant phase element (CPE) is added, that considers the double layer capacitance and the inhomogeneity of the electrode surface. The Warburg element for film modified electrodes is modelled as an open circuit finite Warburg element (Eq. 1) [38,43], which includes parameters A and B.

$$Z(w) = A(w)^{-\frac{1}{2}}(1-\mathrm{j})\coth(B(jw)^{\frac{1}{2}}) \quad (1)$$

A (Eq. 2) es related to the concentration of the electroactive species in the film (C) and the electron diffusion (D), and thus has the same dependence that an infinite Warburg impedance at high frequencies since the system cannot detect the limit of the film in these conditions.

$$A = \frac{RT}{n^2F^2A2^{1/2}}\left[\frac{1}{D_O{}^{1/2}C_O} + \frac{1}{D_R{}^{1/2}C_R}\right] = \frac{RT2^{1/2}}{n^2F^2AD^{1/2}C} \quad (2)$$

working at $E = E^0$, $C_O = C_R = C$, and $D_O \approx D_R = D$.

On the other hand, B (Eq. 3) is related to the ratio between the thickness of the film (d) and the electron diffusion (D).

$$B = \frac{d}{D^{1/2}} \quad (3)$$

Table 4 shows the parameters of EIS analysis and some characteristics of the films formed while Fig. S3B shows the fittings for each experiment.

R_S and R_{CT} are solution and charge transfer resistance. Q_{dl} and n are the parameters describing constant phase element (CPE). A and B are related to the finite open Warburg (Z_W) (Eqs. 1 to 3). Γ, d and D are the coverage surface, thickness of the film and electron diffusion coefficient, respectively. [a]Thickness obtained using Saurbrey model for films with 50% hydration. [b]Calculated from the mass ratio with @Pi matrix for two bilayers (see Table 2). [c]Calculated from Ref [44]. [d]Calculated from parameter B and thickness of the film.

Cyclic voltammetry experiments in the presence of glucose, where osmium centers act as GDH mediator in the oxidation process are depicted in Fig. S2B. The modified electrodes were analyzed in the presence of glucose to study the catalytic response of the systems stabilized by electrostatic (@H_2O), hydrophobic (@NaBr) or hydrogen bond (@Pi or @Pi,HIS) interactions. In the systems with hydrogen bond interactions, current densities increase up to the second bilayer and then a decrease is observed (Fig. 4). Using @Pi as matrix for OsPAA, the catalytic current density reaches 117 μA cm^{-2} for the second bilayer, ca. 20 times the response obtained for the assembly using water. In the presence of NaCl, the catalytic response for the assembly formed is lower (69 μA cm^{-2} for the 2nd layer); even though the electrochemical response in the absence of glucose shows that the amount of OsPAA would be the same (Fig. 3). This may be the case because, as the QCM-D experiments revealed, the bulk of GDH is lost following each polyelectrolyte deposition at high ionic strength. The catalytic current density obtained for the assembly stabilized by hydrophobic interactions (@NaBr) reaches only 6.2 μA cm^{-2} for the first bilayer, compared to 117 μA cm^{-2} for OsPAA@Pi. As the number of bilayers increases, the catalytic behavior is deteriorating, and current densities decreased.

The use of phosphate matrix in OsPAA solutions allows the formation of LbL assemblies with a positive charge enzyme such as GDH. Thus, this type of self-assembly was further evaluated with HRP, which, similarly to GDH at pH 6.1 has a positive surface charge. In the presence of hydrogen peroxide, osmium centers act as HRP mediator in the reduction process, generating a catalytic current density (Fig. S2C).

In the absence of hydrogen peroxide, the assembly with OsPAA@Pi (Fig. 5A) shows a similar behavior to that observed with GDH (Fig. 3) but reaching only 14 μA cm^{-2}. The electrodes modified with OsPAA@Pi and HRP, in the presence of hydrogen peroxide (Fig. 5B), show a higher catalytic current density, which increase linearly up to 3rd bilayer, reaching 323 μA cm^{-2}. In the assembly with OsPAA@Pi,HIS the non-catalytic current densities remain constant while the catalytic current densities decrease with the number of bilayers. These results suggest that the adsorption of HRP is less favored than that of GDH.

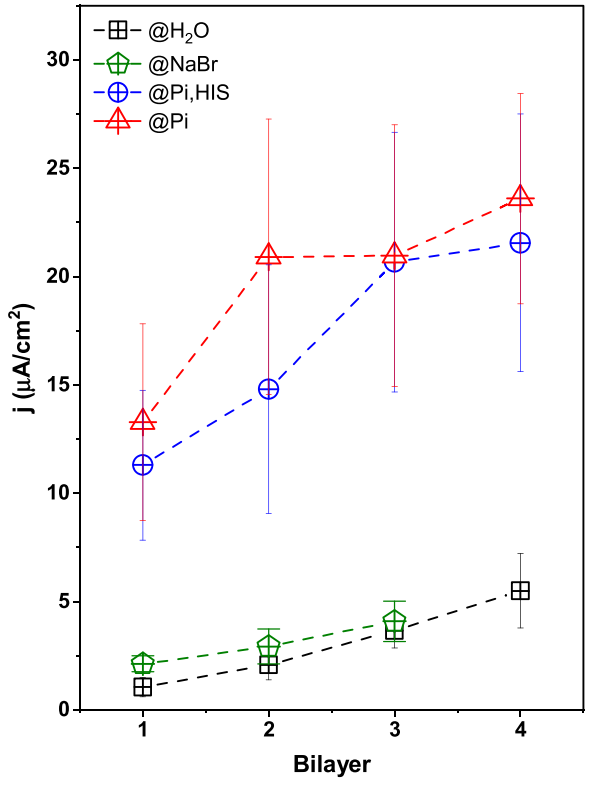

Fig. 3. Peak current densities of cyclic voltammograms after deposition of each bilayer (OsPAA@X/GDH@H_2O) without glucose. Scan rate: 10 mV s^{-1}. Buffer: 50 mM HEPES + 0.1 M NaCl, pH 7.0.

Table 4
Parameters of EIS measurements for modified electrodes using OsPAA in different matrix.

Matrix	R_S (kΩ)	R_{CT} (kΩ)	CPE		Z_W		Γ (nmol cm^{-2})	*d* (nm)	D[d] (cm^2 s^{-1})
			Q_{dl} (Ω^{-1} s^n)	n	A (Ω s$^{-1/2}$)	B (s$^{1/2}$)			
@Pi	0.34	0.38	1.5×10^{-4}	0.72	497	4.0×10^{-2}	2.33	107[a]	7.2×10^{-8}
@Pi,HIS	0.37	0.33	1.1×10^{-4}	0.78	778	4.3×10^{-2}	2.06	54[b]	1.6×10^{-8}
@H_2O	0.28	0.12	2.8×10^{-5}	0.75	1240	3.9×10^{-3}	0.34	25[c]	4.2×10^{-7}

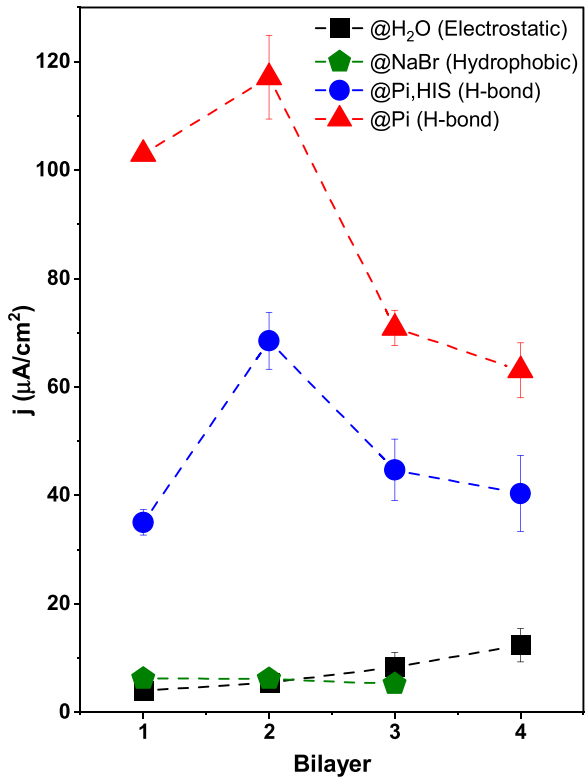

Fig. 4. Maximum catalytic current densities after deposition of each bilayer (OsPAA@X/GDH@H_2O) in the presence of 100 mM glucose. Scan rate: 10 mV s^{-1}. Buffer: 50 mM HEPES + 0.1 M NaCl, pH 7.0.

3.2. One-pot (OP) drop-casting assemblies

We investigated the effect of phosphate (10 mM, pH 6.1) as a crosslinker for both OsPAA and the enzyme (GDH o HRP) with or without 1 M NaCl by casting a drop of these solutions onto an electrode surface to promote spontaneous casting.

DLS measurements show that in the presence of 1 M NaCl no crosslinked particles are formed with GDH or HRP (Table 5). The presence of phosphate ions allows for a unimodal distribution of colloidal particles with GDH (550 nm) and HRP (510 nm). In addition, the absence of free enzyme molecules (4–8 nm) indicates that all of them have been successfully integrated into these particles through phosphate crosslinking. The addition of 1 M NaCl produces the same effect observed for OsPAA solutions (Table 2), the polydispersity increases and smaller colloidal particles (200 nm for GDH and 390 nm for HRP) and the presence of free polymer and/or enzyme (7–10 nm) were observed.

The results of electrochemical measurements with modified electrodes by OP assemblies with GDH are shown in Fig. 6. In the absence of glucose, the system with phosphate reaches a similar non-catalytic current density (29.5 μA cm^{-2}) to that obtained for 4th bilayer in LbL assembly using OsPAA@Pi (23.6 μA cm^{-2}). On the other hand, the current density obtained with the addition of NaCl gets a value of 16.5 μA cm^{-2}, indicating a lower amount of OsPAA adsorbed, and also this current density is lower than the one observed with the LbL assembly. In the presence of glucose, the current density achieved for the system OsPAA@GDH,Pi (87.3 μA cm^{-2}) was higher than that obtained with OsPAA@GDH,Pi,HIS (74.9 μA cm^{-2}).

As well, OP constructs with HRP were evaluated (Fig. 7). In the absence of hydrogen peroxide, a greater current density is obtained for the OsPAA@HRP,Pi system, reaching 95 μA cm^{-2}. In the presence of hydrogen peroxide, a similar catalytic current density is obtained for OsPAA@HRP,Pi (354 μA cm^{-2}) in comparison to the OsPAA@Pi/HRP LbL assembly (323 μA cm^{-2} for the 3rd bilayer). For OsPAA@HRP,Pi, HIS, the catalytic current density only reaches a value less than one tenth of the current density (see Fig. 7).

4. Discussion

The interaction between phosphate ions and polyamines allows the formation of stable colloidal particles. Depending on the concentration of these species, pH, and ionic strength, their adsorption or desorption on surfaces and the formation of assemblies with enzymes can be tuned [19,41,45].

Hydrogen bond interactions with primary amines cause the redox polyelectolyte's conformation to change in the presence of phosphate ions, resulting in the creation of globular structures [19]. An increase in ionic strength up to 1 M NaCl, produce a highly polydisperse mixture of smaller particles (Table 2). Furthermore, not all the polyelectrolyte forms these particles, some of them retaining a random-coil structure similar to that in the absence of phosphate. The OsPAA particles forming by phosphate ions are adsorbed on a gold surface (AFM experiments) with a higher coverage compared to a random-coil conformation. With the adsorption of GDH, the distribution of these globular structures is evidenced by a thicker and rougher film with respect to the absence of crosslinker ion (Fig. 2 and S1), based on this analysis we proposed the Scheme 2 which represent the assemblies obtained from the different matrixes.

The formation of these redox particles allows for a higher adsorption on graphite forming a film on which an enzyme can be adsorbed. This last adsorption process will depend on the interactions between the redox polyelectrolyte film and the enzyme, as well as entropic factors. Using a positive enzyme such as GDH, electrostatic interactions are not favored. However, the presence of phosphate ions causes a change in the polyelectrolyte configuration, allowing interaction with the enzyme's arginine and lysine residues [34,41,46,47].

Microgravimetric measurements (Fig. 1) show that the growth of the polyelectrolyte/phosphate-enzyme assembly is affected by the ionic strength. At low ionic strength, both species are readily adsorbed, while at high ionic strength, a more complex phenomenon is observed. Even though the enzyme can be adsorbed on the polyelectrolyte, in the next step, the OsPAA@Pi,HIS solution removes part of the adsorbed mass, suggesting that OsPAA was not adsorbed and GDH was removed from the surface. However, electrochemical analysis showed an increase in the current density response with the number of bilayers (Fig. 3), which is associated with more OsPAA adsorbed in each deposition step. A similar behavior to the assembly with OsPAA@Pi,HIS was previously obtained with the use of hydrophobic anions [24], where it was demonstrated that the decrease in adsorbed mass is a balance between the removal of the enzyme and the deposition of the electroactive

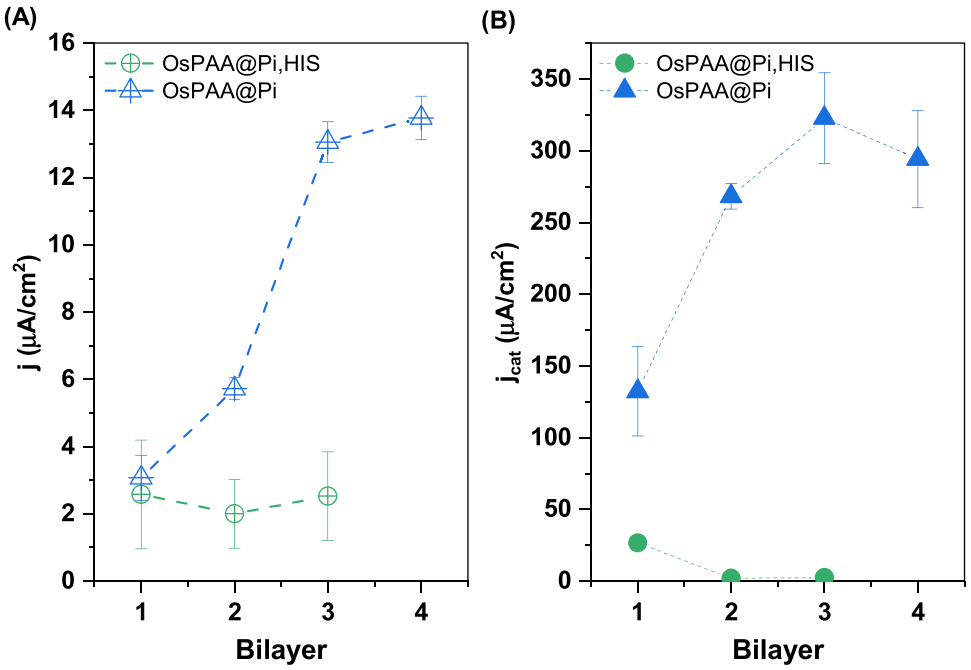

Fig. 5. (A) Peak current densities of cyclic voltammograms after deposition of each bilayer (OsPEI@X/HRP@H2O) without hydrogen peroxide. (B) Maximum catalytic current densities in the presence of 2 mM H_2O_2. Scan rate: 10 mV s^{-1}. Buffer: 50 mM Acetate + 0.15 M NaCl, pH 5.0.

Table 5
OsPAA and enzyme solutions studied by Dynamic Light Scattering (DLS).

Samples[a]	Diameter (nm)	PLD	Zeta potential (mV)
@GDH,HIS	8 ± 2	0.9	BAT[b]
@GDH,Pi	550 ± 50	0.5	BAT[b]
@GDH,Pi,HIS	10 ± 4	0.9	-2
	200 ± 80		
@HRP,HIS	4 ± 1	0.6	+ 15
@HRP,Pi	510 ± 10	0.2	+ 11
@HRP,Pi,HIS	7 ± 1	0.3	+ 10
	390 ± 40		

[a] @Enzyme,X followed the same nomenclature as described on Table 1 with GDH or HRP at final concentration 2 mg mL^{-1}.
[b] Below the acceptable threshold.

polyelectrolyte.

Although Fig. 3 suggests that there is not a large effect due to ionic strength on the electrochemical response of osmium centers adsorbed, DLS measurements show that the addition of 1 M NaCl induces the destabilization of the colloidal particles, reducing its size, and leaving free OsPAA which can be easily rinsed from the electrode surface. The presence of a high concentration of chloride disturbed the interaction between the polyelectrolyte and the phosphate ions. Here, the ion pairing between chloride and amino groups competes with the phosphate-amine interaction, generating a system with a more hydrophobic character that displaces the proteins from the film to introduce more electroactive polyelectrolyte, as shown in the electrochemical results, where, in the absence of glucose, the system has a response similar to the one built in the presence of only phosphate, but in the presence of glucose, the signal is poorer.

If we only consider electrostatic interactions, the formation of OsPAA/GDH self-assembly should not be favored. However, using water as matrix, a layer-by-layer assembly with components of equal charge was built, showing that the systems is stabilized by other interactions and entropic factors [15,48–50]. When phosphate ions are present, the formed particles not only allow for more adsorbed OsPAA, but also for more GDH adsorption. This can be due to the fact that the colloidal particles have a charge surface close to zero (see Table 2), which reduces

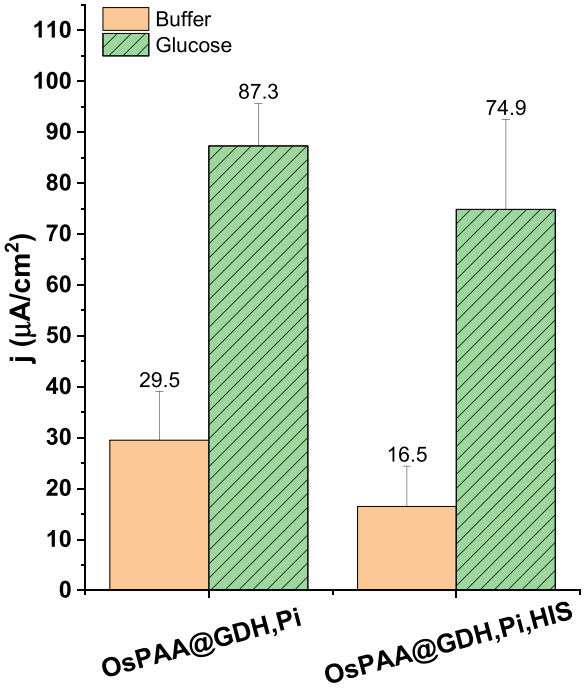

Fig. 6. Current densities for cyclic voltammetries carried out at 10 mV s^{-1} performed in 50 mM HEPES buffer + 0.1 M NaCl, pH 7.0 (filled) and in the presence of 100 mM Glucose in the same buffer (black lines) for different matrices with GDH.

the electrostatic repulsion with the enzyme, and that phosphate ions can interact with amino acids from the enzyme by hydrogen bond interactions or enhance hydrophobic interactions [34,41,46,47].

To evaluate the effect of hydrophobic interactions between GDH and OsPAA, we performed an experiment using OsPAA in the presence of 0.2 M NaBr (@NaBr, Fig. 3). Bromide ions through ion pairing introduce a stronger hydrophobic character in the polymeric chains of OsPAA

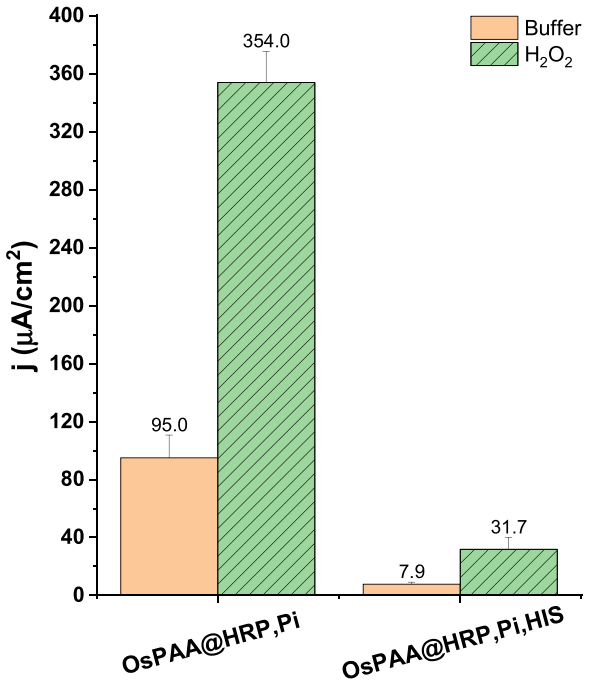

Fig. 7. Current densities for cyclic voltammetries carried out at 10 mV s^{-1} performed in 50 mM acetate buffer + 0.15 M NaCl, pH 5.0 (filled) and in the presence of 2 mM H_2O_2 in the same buffer (black lines) for different matrices with HRP.

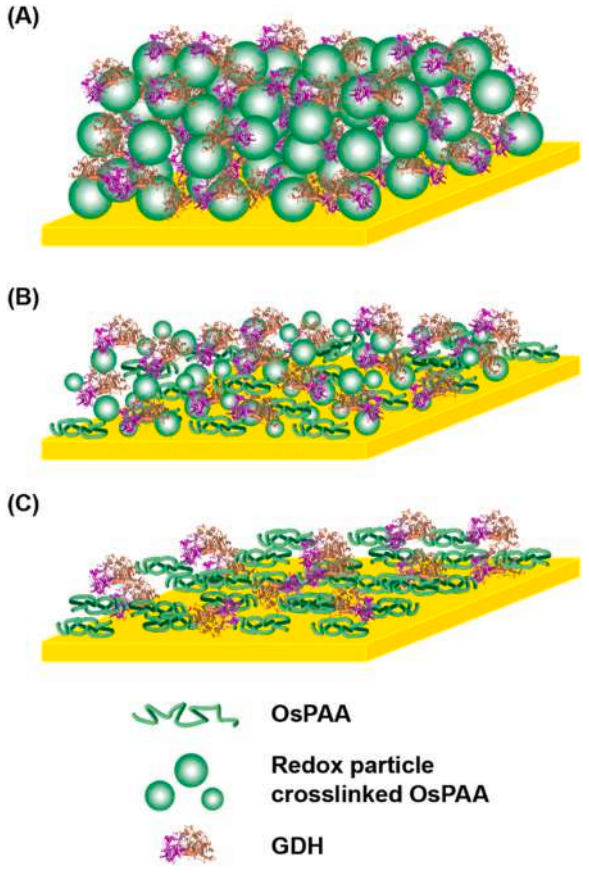

Scheme 2. Description of modified surfaces via LbL self-assembly process using GDH and OsPAA as (A) unimodal redox particles in @Pi matrix, (B) bimodal smaller redox particles in @Pi,HIS matrix and (C) random-coil in @H_2O.

enhancing the hydrophobic interaction with the enzyme [24]. The current response in the absence of glucose increases with the number of bilayer and is slightly higher in comparison with water as a matrix. The non-catalytic response of this system shows that hydrophobic interactions between OsPAA and GDH are poor and has no consequences in the assembly buildup.

EIS measurements allow the analysis of the current propagation through the film [38,51,52]. Each film was analyzed by fitting an equivalent circuit (Fig. S3A). The main differences among the films can be observed in the values of the constant phase element (CPE) and open Warburg element (A and B) that are related to the physical characteristics of the film. CPE is an order of magnitude higher for the systems built in the presence of phosphate, that can be related to a more compact film and therefore a higher concentration of ions. With respect to the B parameter, related to the thickness/diffusion ratio (Eq. 3), the film grown in water presents a smaller value than the others, in agreement to the amount of mass adsorbed on the surface. All the films have *D* in the order of 10^{-7}-10^{-8} cm^2 s^{-1} in agreement with early results for this type of electroactive polyelectrolytes, [37] meaning that the presence of phosphate allows the adsorption of a higher amount of material maintaining an efficient electron diffusion in thicker films. On the other hand, R_S, considers primarily the solution's resistance, which is always the same, and R_{CT}, the charge transfer related to the ability of the redox centers to exchange electrons with the surface, yielding similar results in all cases studied.

The modified electrodes were evaluated by cyclic voltammetry at several scan rates ranging from 2 to 500 mV s^{-1} in buffer solution. From these voltammetries, peak currents of anodic and cathodic process were obtained. Log (i_p) vs Log (v) (Fig. S4A) shows a linear dependency with slopes near one unit for the three systems, which indicates that charge is propagated fast enough to not be limited by diffusion. All the systems present some degree of repulsion since the widths of the current peaks at half-height are broader than 90 mV (Fig. S4B), the @Pi system show a value slightly smaller probably due to the chains of the polyelectrolyte are bound through phosphate ions balancing the charge repulsion [53, 54].

Regarding the catalytic process, a higher catalytic and non-catalytic current density ratio (j_c/j_0) demonstrates an effective electron transfer between redox centers of mediator and enzyme. The assemblies stabilized by hydrogen bond (@Pi or @Pi,HIS) showed a higher maximum value compared to the system stabilized by electrostatic interactions. Nevertheless, at high ionic strength, the catalytic response decreases, this can be explained by the smaller amount of enzyme incorporated to the electrode, as the microgravimetry results suggested. The assembly with phosphate gets a j_c/j_0 of 5.6, while with the addition of NaCl this value decreases up to 4.6 and only reach 2.6 for the assembly with water. These results reveal that the colloidal particles formed by the presence of phosphate ions is the main driving force to assemble the positive GDH.

As well as the non-catalytic current was analyzed for the assembly stabilized by hydrophobic interactions, the response in the presence of glucose using @NaBr as OsPAA matrix was evaluated. The catalytic response of this system shows that although hydrophobic interactions were enhanced, they do not improve in the enzyme adsorption as it was previously observed for glucose oxidase, [24] an issue that deserves a more detailed study regarding the hydrophobic/hydrophilic surfaces of both enzymes.

The performance of these LbL systems using phosphate as matrix were evaluated for HRP immobilization, another enzyme with high pI and relevant for biotechnological applications. The current densities in the absence of hydrogen peroxide for the assembly with @Pi matrix (Fig. 5A) increases with each bilayer following a similar behavior observed for the assemblies with GDH (Fig. 3). However, the maximum current density with GDH reaches ca. 2 times than with HRP (24 vs 14 μA cm^{-2}). These results suggest that OsPAA adsorption on HRP is less favored than on GDH. This difference could be explained by the fact that

GDH surfaces are more evenly distributed with basic aminoacids like lysine and arginine, which can create hydrogen bridges with phosphate ions found in OsPAA particles (Fig. S5) [47]. Furthermore, in the presence of hydrogen peroxide, this system gets a j_c/j_0 ratio of 25 for the 3rd bilayer, 4.5 times higher than the ratio obtained for OsPAA/GDH assembly (5.6 for the 2nd bilayer), showing that despite a lower OsPAA adsorbed, the formed film reveal a more effective electron transfer with the active site of HRP and the higher catalytic turnover of this enzyme. In contrast to GDH, the assembly with OsPAA@Pi,HIS exhibits poor non-catalytic current densities (2.5 μA cm^{-2}) and remains constant. OsPAA@Pi,HIS, particles were unable to adsorb on HRP attributable to fewer amino acids available to interact with phosphate and then can be easily rinsed and as a consequence catalytic currents are not observed (Fig. 4B).

Recently, the formation of enzyme-polymer complexes (EPC) has been studied as an alternative that allows to avoid electrostatic repulsion between enzyme and polymer. EPC is formed by electrostatic interaction using a polyanion which surrounds a positive charged surface enzyme, standardizing its charge. Then, this EPC could be self-assembled with a polycation that interacts with the EPC forming an electrostatic LbL. This was evaluated for different proteins such as lysozyme, insulin and glucose oxidase with several polyanions and polycations [16,55]. Here, we proposed an alternative methodology to electrostatic LbL assembly, simply with an addition of a multivalent anion able to crosslink the polycation to form redox particles, screening the electrostatic interactions as is indicated by the low Z-potential, and capable to interact with amino acids on the enzyme surface by hydrogen bond interactions.

OP self-assembly technique is an easy and quick option to modify several types of surfaces with macromolecules. Since phosphate ions can act as amino crosslinker group, enzymatic-polyelectrolyte electroactive particles can be formed [34]. Redox particles formed using @GDH,Pi and @GDH,Pi,HIS were deposited on the electrode surface and evaluated in the presence and in the absence of glucose. In the absence of glucose, the system with phosphate reaches a higher non-catalytic current density to the obtained for 4th bilayer in LbL assembly using OsPAA@Pi. In the presence of glucose, the current density achieved using @GDH,Pi matrix was higher although the j_c/j_0 ratio was lower reaching a value of 3. These findings show that the OP approach is a quick and effective means of immobilizing a significant amount of polyelectrolyte, but that the enzyme retention or interaction in the produced film is less satisfactory. On the other hand, the addition of NaCl indicates a less amount of OsPAA adsorbed ay high ionic strength and a poor catalytic current density compared to the results obtained in the absence of NaCl.

As in the case of LbL assemblies, OP technique was also evaluated for HRP and OsPAA immobilization. This self-assembly methodology allows to incorporate a higher amount of OsPAA on the electrode surface using @Pi matrix related to non-catalytic current density, in comparison to LbL technique (95 μA cm^{-2} for OP vs 14 μA cm^{-2} for LbL assembly). Nevertheless, a similar catalytic current density is obtained in comparison to LbL assembly using the same matrix. Non-catalytic and catalytic current densities in films generated in the presence of NaCl only reach values less than one tenth of the current density obtained without NaCl. The similarity observed with the addition of NaCl for both enzymes indicates that an important part of the material does not form particles and they are easily removed by rinsing. Although a slightly higher catalytic current for HRP immobilization is achieved by OP, the ratio j_c/j_0 equals 25 indicates that the LbL technique is the more efficient process to assemble this enzyme to enhance the electron transfer with OsPAA.

5. Conclusions

In this work, we presented and alternative methodology for the construction of polyamine-protein assemblies regardless the protein charge used in the construction process taking advantage of the ability of amino groups, present in the polyelectrolyte and the enzymes, to form hydrogen bonds with phosphate ions, acting as effective crosslinking agent.

Two assembly techniques were used, layer by layer, which allows a molecular control of the material adsorbed on the electrode and a more detailed analysis of the results, and one-pot drop-casting, which represents a quick and simple way to build this kind of systems, both showing excellent catalytic behavior. For example, the currents obtained with the layer by layer with GDH are similar to those obtained by GOx in the presence of phosphate ions [41] or surfactants [5]. On the other hand, HRP was previously adsorbed on a electroactive polyamine by glycosylation of the polyelectrolyte and using as crosslinking agent an osmium derivatized concanavalin A, able to be bound the glycosylated polyelectrolyte and a glycosylated protein, exemplified by HRP and obtaining maximum catalytic currents in the order of 100 μA cm^{-2} [56,57] while in this work are in the order of 300 with a simpler experimental procedure.

The results presented here introduced a novel strategy that broaden the range of options to build electroactive-enzyme films and can be extended in the development of immobilized enzyme biocatalysts [58].

Funding

Fernando Battaglini received funding from ANPCYT, Argentina (PRESTAMO BID-PICT NRO 2018–02075), Universidad de Buenos Aires (UBACYT Grant 0020170100341BA) and CONICET (Grant KE5 11220200101473CO).

CRediT authorship contribution statement

Lucy L. Coria-Oriundo: Conceptualization, Investigation, Methodology, Formal analysis, Writing – original draft. **M. Lorena Cortez:** Conceptualization, Methodology, Formal analysis. **Santiago E. Herrera:** Conceptualization, Methodology, Formal analysis. **Omar Azzaroni:** Conceptualization, Methodology, Formal analysis. **Fernando Battaglini:** Conceptualization, Formal analysis, Supervision, Writing – review & editing.

Declaration of Competing Interest

The authors declare that they have no known competing financial interests or personal relationships that could have appeared to influence the work reported in this paper.

Data Availability

Data will be made available on request.

Appendix A. Supporting information

Supplementary data associated with this article can be found in the online version at doi:10.1016/j.synthmet.2023.117308.

References

[1] J. Fu, J.B. Schlenoff, Driving forces for oppositely charged polyion association in aqueous solutions: enthalpic, entropic, but not electrostatic, J. Am. Chem. Soc. 138 (2016) 980–990, https://doi.org/10.1021/jacs.5b11878.

[2] J. Irigoyen, S.E. Moya, J.J. Iturri, I. Llarena, O. Azzaroni, E. Donath, Specific ζ-potential response of layer-by-layer coated colloidal particles triggered by polyelectrolyte ion interactions, Langmuir 25 (2009) 3374–3380, https://doi.org/10.1021/LA803360N/ASSET/IMAGES/MEDIUM/LA-2008-03360N_0010.GIF.

[3] G. Pérez-Mitta, W.A. Marmisollé, A.G. Albesa, M.E. Toimil-Molares, C. Trautmann, O. Azzaroni, Phosphate-responsive biomimetic nanofluidic diodes regulated by polyamine–phosphate interactions: insights into their functional behavior from theory and experiment, Small 14 (2018), 1702131, https://doi.org/10.1002/SMLL.201702131.

[4] M.L. Cortez, W. Marmisollé, D. Pallarola, L.I. Pietrasanta, D.H. Murgida, M. Ceolín, O. Azzaroni, F. Battaglini, Effect of gold nanoparticles on the structure and electron-transfer characteristics of glucose oxidase redox polyelectrolyte-surfactant

complexes, Chem. A Eur. J. 20 (2014) 13366–13374, https://doi.org/10.1002/chem.201402707.
[5] M.L. Cortez, M. Ceolín, L.C. Camacho, E. Donath, S.E. Moya, F. Battaglini, O. Azzaroni, Solvent effects on the structure–property relationship of redox-active self-assembled nanoparticle–polyelectrolyte–surfactant composite thin films: implications for the generation of bioelectrocatalytic signals in enzyme-containing assemblies, ACS Appl. Mater. Interfaces 9 (2017) 1119–1128, https://doi.org/10.1021/acsami.6b13456.
[6] M.L. Cortez, M. Ceolín, O. Azzaroni, F. Battaglini, Formation of redox-active self-assembled polyelectrolyte–surfactant complexes integrating glucose oxidase on electrodes: Influence of the self-assembly solvent on the signal generation, Bioelectrochemistry 105 (2015) 117–122, https://doi.org/10.1016/j.bioelechem.2015.06.001.
[7] M. Lorena Cortez, N. de Matteis, M. Ceolín, W. Knoll, F. Battaglini, O. Azzaroni, Hydrophobic interactions leading to a complex interplay between bioelectrocatalytic properties and multilayer meso-organization in layer-by-layer assemblies, Phys. Chem. Chem. Phys. 16 (2014) 20844–20855, https://doi.org/10.1039/C4CP02334J.
[8] T. Berninger, C. Bliem, E. Piccinini, O. Azzaroni, W. Knoll, Cascading reaction of arginase and urease on a graphene-based FET for ultrasensitive, real-time detection of arginine, Biosens. Bioelectron. 115 (2018) 104–110, https://doi.org/10.1016/j.bios.2018.05.027.
[9] G.E. Fenoy, E. Piccinini, W. Knoll, W.A. Marmisollé, O. Azzaroni, The effect of amino–phosphate interactions on the biosensing performance of enzymatic graphene field-effect transistors, Anal. Chem. 94 (2022) 13820–13828, https://doi.org/10.1021/acs.analchem.2c02373.
[10] Y. Toum Terrones, G. Laucirica, V.M. Cayón, G.E. Fenoy, M.L. Cortez, M.E. Toimil-Molares, C. Trautmann, W.A. Mamisollé, O. Azzaroni, Highly sensitive acetylcholine biosensing via chemical amplification of enzymatic processes in nanochannels, Chem. Commun. 58 (2022) 10166–10169, https://doi.org/10.1039/D2CC02249D.
[11] E. Piccinini, C. Bliem, C. Reiner-Rozman, F. Battaglini, O. Azzaroni, W. Knoll, Enzyme-polyelectrolyte multilayer assemblies on reduced graphene oxide field-effect transistors for biosensing applications, Biosens. Bioelectron. 92 (2017) 661–667, https://doi.org/10.1016/j.bios.2016.10.035.
[12] G. Pérez-Mitta, A.S. Peinetti, M.L. Cortez, M.E. Toimil-Molares, C. Trautmann, O. Azzaroni, Highly sensitive biosensing with solid-state nanopores displaying enzymatically reconfigurable rectification properties, Nano Lett. 18 (2018) 3303–3310, https://doi.org/10.1021/ACS.NANOLETT.8B01281/SUPPL_FILE/NL8B01281_SI_001.PDF.
[13] C.M.A. Brett, Perspectives and challenges for self-assembled layer-by-layer biosensor and biomaterial architectures, Curr. Opin. Electrochem. 12 (2018) 21–26, https://doi.org/10.1016/j.coelec.2018.11.004.
[14] F. Lisdat, Trends in the layer-by-layer assembly of redox proteins and enzymes in bioelectrochemistry, Curr. Opin. Electrochem. 5 (2017) 165–172, https://doi.org/10.1016/j.coelec.2017.09.002.
[15] J. Zhang, X. Huang, L. Zhang, Y. Si, S. Guo, H. Su, J. Liu, Layer-by-layer assembly for immobilizing enzymes in enzymatic biofuel cells, Sustain Energy Fuels 4 (2020) 68–79, https://doi.org/10.1039/C9SE00643E.
[16] C. Vranckx, L. Lambricht, V. Préat, O. Cornu, C. Dupont-Gillain, A. vander Straeten, Layer-by-layer nanoarchitectonics using protein–polyelectrolyte complexes toward a generalizable tool for protein surface immobilization, Langmuir 38 (2022) 5579–5589, https://doi.org/10.1021/acs.langmuir.2c00191.
[17] L. D'Agostino, M. di Pietro, A. di Luccia, Nuclear aggregates of polyamines are supramolecular structures that play a crucial role in genomic DNA protection and conformation, FEBS J. 272 (2005) 3777–3787, https://doi.org/10.1111/j.1742-4658.2005.04782.x.
[18] A. Lopera, J.A. Aguilar, R. Belda, B. Verdejo, J.W. Steed, E. García-España, Hybrid GMP–polyamine hydrogels as new biocompatible materials for drug encapsulation, Soft Matter 16 (2020) 6514–6522, https://doi.org/10.1039/D0SM00704H.
[19] S.E. Herrera, M.L. Agazzi, M.L. Cortez, W.A. Marmisollé, M. Tagliazucchi, O. Azzaroni, Polyamine colloids cross-linked with phosphate ions: towards understanding the solution phase behavior, ChemPhysChem 20 (2019) 1044–1053, https://doi.org/10.1002/cphc.201900046.
[20] M.L. Agazzi, S.E. Herrera, M.L. Cortez, W.A. Marmisollé, O. Azzaroni, Self-assembled peptide dendrigraft supraparticles with potential application in pH/enzyme-triggered multistage drug release, Colloids Surf. B Biointerfaces 190 (2020), https://doi.org/10.1016/J.COLSURFB.2020.110895.
[21] M.L. Agazzi, S.E. Herrera, M.L. Cortez, W.A. Marmisollé, M. Tagliazucchi, O. Azzaroni, Insulin delivery from glucose-responsive, self-assembled, polyamine nanoparticles: smart "sense-and-treat" nanocarriers made easy, Chem. – A Eur. J. 26 (2020) 2456–2463, https://doi.org/10.1002/chem.201905075.
[22] S.E. Herrera, M.L. Agazzi, M.L. Cortez, W.A. Marmisollé, C. Bilderling, O. Azzaroni, Layer-by-layer formation of polyamine-salt aggregate/polyelectrolyte multilayers. loading and controlled release of probe molecules from self-assembled supramolecular networks, Macromol. Chem. Phys. 220 (2019), 1900094, https://doi.org/10.1002/macp.201900094.
[23] M.L. Agazzi, S.E. Herrera, M.L. Cortez, W.A. Marmisollé, C. von Bilderling, L. I. Pietrasanta, O. Azzaroni, Continuous assembly of supramolecular polyamine-phosphate networks on surfaces: Preparation and permeability properties of nanofilms, Soft Matter 15 (2019) 1640–1650, https://doi.org/10.1039/c8sm02387e.
[24] L.L. Coria-Oriundo, S.E. Herrera, L.P. Méndez De Leo, F. Battaglini, Current response enhancement according to the doping anion's nature in redox polyelectrolyte-enzyme assemblies, ACS Appl. Polym. Mater. (2022), https://doi.org/10.1021/acsapm.2c01300.
[25] M. Pál, G. Szalai, O.K. Gondor, T. Janda, Unfinished story of polyamines: Role of conjugation, transport and light-related regulation in the polyamine metabolism in plants, Plant Sci. 308 (2021), 110923, https://doi.org/10.1016/j.plantsci.2021.110923.
[26] C.H. Kwon, Y. Ko, D. Shin, M. Kwon, J. Park, W.K. Bae, S.W. Lee, J. Cho, High-power hybrid biofuel cells using layer-by-layer assembled glucose oxidase-coated metallic cotton fibers, Nat. Commun. 9 (2018) 4479, https://doi.org/10.1038/s41467-018-06994-5.
[27] M. He, F. Chen, D. Shao, P. Weis, Z. Wei, W. Sun, Photoresponsive metallopolymer nanoparticles for cancer theranostics, Biomaterials 275 (2021), 120915, https://doi.org/10.1016/j.biomaterials.2021.120915.
[28] Y. Wang, D. Astruc, A.S. Abd-El-Aziz, Metallopolymers for advanced sustainable applications, Chem. Soc. Rev. 48 (2019) 558–636, https://doi.org/10.1039/C7CS00656J.
[29] H. Xiao, L. Yan, E.M. Dempsey, W. Song, R. Qi, W. Li, Y. Huang, X. Jing, D. Zhou, J. Ding, X. Chen, Recent progress in polymer-based platinum drug delivery systems, Prog. Polym. Sci. 87 (2018) 70–106, https://doi.org/10.1016/j.progpolymsci.2018.07.004.
[30] A. Heller, B. Feldman, Electrochemistry in diabetes management, Acc. Chem. Res 43 (2010) 963–973, https://doi.org/10.1021/ar9002015.
[31] P.N. Bartlett, C.S. Toh, E.J. Calvo, V. Flexer, Modelling biosensor responses, in: Bioelectrochemistry: Fundamentals, Experimental Techniques and Applications, Wiley, Chichester, England, 2008, pp. 267–325.
[32] E.J. Calvo, R. Etchenique, L. Pietrasanta, A. Wolosiuk, C. Danilowicz, Layer-by-layer self-assembly of glucose oxidase and Os(Bpy) $_2$ ClPyCH $_2$ NH−poly (Allylamine) bioelectrode, Anal. Chem. 73 (2001) 1161–1168, https://doi.org/10.1021/ac0011686.
[33] N.P. Godman, J.L. DeLuca, S.R. McCollum, D.W. Schmidtke, D.T. Glatzhofer, Electrochemical characterization of layer-by-layer assembled ferrocene-modified linear poly(ethylenimine)/enzyme bioanodes for glucose sensor and biofuel cell applications, Langmuir 32 (2016) 3541–3551, https://doi.org/10.1021/acs.langmuir.5b04753.
[34] L.L. Coria-Oriundo, M.L. Cortez, O. Azzaroni, F. Battaglini, Enzymes hosted in redox-active ionically cross-linked polyelectrolyte networks enable more efficient biofuel cells, Soft Matter 17 (2021) 5240–5247, https://doi.org/10.1039/D1SM00221J.
[35] T.J. Ohara, R. Rajagopalan, A. Heller, Glucose electrodes based on cross-linked [Os(bpy)2Cl]+/2+ complexed Poly(1-vinylimidazole) films, Anal. Chem. 65 (1993) 3512–3517, https://doi.org/10.1021/ac00071a031.
[36] V. Flexer, N. Mano, Wired pyrroloquinoline quinone soluble glucose dehydrogenase enzyme electrodes operating at unprecedented low redox potential, Anal. Chem. 86 (2014) 2465–2473, https://doi.org/10.1021/ac403334w.
[37] H. Larsson, M. Sharp, Charge propagation in [Os(bpy)2(PVP)xCl]Cl polymers. An example of mean field behavior in a system with constrained diffusion of redox sites? J. Electroanal. Chem. 381 (1995) 133–142, https://doi.org/10.1016/0022-0728(94)03654-L.
[38] R. Pauliukaite, M.E. Ghica, O. Fatibello-Filho, C.M.A. Brett, Electrochemical impedance studies of chitosan-modified electrodes for application in electrochemical sensors and biosensors, Electro Acta 55 (2010) 6239–6247, https://doi.org/10.1016/j.electacta.2009.09.055.
[39] G. Levin, F. Mendive, H.M. Targovnik, O. Cascone, M. v Miranda, Genetically engineered horseradish peroxidase for facilitated purification from baculovirus cultures by cation-exchange chromatography, J. Biotechnol. 118 (2005) 363–369, https://doi.org/10.1016/j.jbiotec.2005.05.015.
[40] G. Priano, G. González, M. Günther, F. Battaglini, Disposable gold electrode array for simultaneous electrochemical studies, Electroanalysis 20 (2008) 91–97, https://doi.org/10.1002/elan.200704061.
[41] D. Zappi, L.L. Coria-Oriundo, E. Piccinini, M. Gramajo, C. von Bilderling, L. I. Pietrasanta, O. Azzaroni, F. Battaglini, The effect of ionic strength and phosphate ions on the construction of redox polyelectrolyte-enzyme self-assemblies, Phys. Chem. Chem. Phys. 21 (2019), https://doi.org/10.1039/c9cp04037d.
[42] L. Maldonado, S.E. Herrera, F.J. Williams, M. Tagliazucchi, Thickness fluctuations produce apparent long-range tunneling in large-area junctions: the case of polyelectrolyte multilayers, J. Phys. Chem. C. 126 (2022) 9956–9964, https://doi.org/10.1021/acs.jpcc.2c02175.
[43] J. Pillay, K.I. Ozoemena, Electrochemical properties of surface-confined films of single-walled carbon nanotubes functionalised with cobalt(II)tetra-aminophthalocyanine: Electrocatalysis of sulfhydryl degradation products of V-type nerve agents, Electro Acta 52 (2007) 3630–3640, https://doi.org/10.1016/j.electacta.2006.10.022.
[44] M.L. Cortez, A.L. Cukierman, F. Battaglini, Surfactant presence in a multilayer polyelectrolyte–enzyme system improves its catalytic response, Electrochem Commun. 11 (2009) 990–993, https://doi.org/10.1016/j.elecom.2009.02.041.
[45] G. Laucirica, W.A. Marmisollé, O. Azzaroni, Dangerous liaisons: anion-induced protonation in phosphate-polyamine interactions and their implications for the charge states of biologically relevant surfaces, Phys. Chem. Chem. Phys. 19 (2017) 8612–8620, https://doi.org/10.1039/c6cp08793k.
[46] A.S. Woods, The mighty arginine, the stable quaternary amines, the powerful aromatics, and the aggressive phosphate: their role in the noncovalent minuet, J. Proteome Res. 3 (2004) 478–484, https://doi.org/10.1021/pr0340911.
[47] K.A. Schug, W. Lindner, Noncovalent binding between guanidinium and anionic groups: focus on biological-and synthetic-based arginine/guanidinium interactions with phosph[on]ate and sulf[on]ate residues, Chem. Rev. 105 (2005) 67–113, https://doi.org/10.1021/cr040603j.
[48] G. Zeng, Y. Xing, J. Gao, Z. Wang, X. Zhang, Unconventional layer-by-layer assembly of graphene multilayer films for enzyme-based glucose and maltose

biosensing, Langmuir 26 (2010) 15022–15026, https://doi.org/10.1021/la102806v.
[49] A. Rodriguez-Abetxuko, D. Sánchez-deAlcázar, A.L. Cortajarena, A. Beloqui, A versatile approach for the assembly of highly tunable biocatalytic thin films, Adv. Mater. Interfaces 6 (2019), 1900598, https://doi.org/10.1002/admi.201900598.
[50] E. Guzmán, F. Ortega, R.G. Rubio, Layer-by-layer materials for the fabrication of devices with electrochemical applications, Energy 15 (2022) 3399, https://doi.org/10.3390/en15093399.
[51] M. Tagliazucchi, D. Grumelli, E.J. Calvo, Nanostructured modified electrodes: Role of ions and solvent flux in redox active polyelectrolyte multilayer films, Phys. Chem. Chem. Phys. 8 (2006) 5086–5095, https://doi.org/10.1039/b609341h.
[52] T.A. Silva, A. Wong, O. Fatibello-Filho, Electrochemical sensor based on ionic liquid and carbon black for voltammetric determination of Allura red colorant at nanomolar levels in soft drink powders, Talanta 209 (2020), 120588, https://doi.org/10.1016/j.talanta.2019.120588.
[53] S. Majdi, A. Jabbari, H. Heli, A.A. Moosavi-Movahedi, Electrocatalytic oxidation of some amino acids on a nickel–curcumin complex modified glassy carbon electrode, Electro Acta 52 (2007) 4622–4629, https://doi.org/10.1016/j.electacta.2007.01.022.
[54] A.J. Bard, L.R. Faulkner, Electroactive layers and modified electrodes, in: Electrochemical Methods: Fundamentals and Applications, 2nd ed..,, John Wiley & Sons Inc, 2001, pp. 580–631.
[55] A. vander Straeten, A. Bratek-Skicki, A.M. Jonas, C.-A. Fustin, C. Dupont-Gillain, Integrating proteins in layer-by-layer assemblies independently of their electrical charge, ACS Nano 12 (2018) 8372–8381, https://doi.org/10.1021/acsnano.8b03710.
[56] M.L. Cortez, D. Pallarola, M. Ceolín, O. Azzaroni, F. Battaglini, Ionic self-assembly of electroactive biorecognizable units: Electrical contacting of redox glycoenzymes made easy, Chem. Commun. 48 (2012) 10868–10870, https://doi.org/10.1039/c2cc35949a.
[57] M.L. Cortez, D. Pallarola, M. Ceolín, O. Azzaroni, F. Battaglini, Electron transfer properties of dual self-assembled architectures based on specific recognition and electrostatic driving forces: Its application to control substrate inhibition in horseradish peroxidase-based sensors, Anal. Chem. 85 (2013) 2414–2422, https://doi.org/10.1021/ac303424t.
[58] J.J. Virgen-Ortíz, J.C.S. dos Santos, Á. Berenguer-Murcia, O. Barbosa, R. C. Rodrigues, R. Fernandez-Lafuente, Polyethylenimine: a very useful ionic polymer in the design of immobilized enzyme biocatalysts, J. Mater. Chem. B 5 (2017) 7461–7490, https://doi.org/10.1039/c7tb01639e.